



CHORUS

This is the accepted manuscript made available via CHORUS. The article has been published as:

Operator product expansion beyond leading order for two-component fermions

Samuel B. Emmons, Daekyoung Kang, and Lucas Platter

Phys. Rev. A **94**, 043615 — Published 10 October 2016

DOI: [10.1103/PhysRevA.94.043615](https://doi.org/10.1103/PhysRevA.94.043615)

The Operator Product Expansion Beyond Leading Order for Two-Component Fermions

Samuel B. Emmons,^{1,*} Daekyoung Kang,^{2,†} and Lucas Platter^{1,3,‡}

¹*Department of Physics and Astronomy, University of Tennessee, Knoxville, TN 37996, USA*

²*Theoretical Division, MS B283, Los Alamos National Laboratory, Los Alamos, NM 87545, USA*

³*Physics Division, Oak Ridge National Laboratory, Oak Ridge, TN 37831, USA*

We consider a homogeneous, balanced gas of strongly interacting fermions in two spin states interacting through a large scattering length. Finite range corrections are needed for a quantitative description of data which experiments and numerical simulations have provided. We use a perturbative field theoretical framework and a tool called the Operator Product Expansion (OPE), which together allow for the expression of finite range corrections to the universal relations and momentum distribution. Using the OPE, we derive the $1/k^6$ part of the momentum tail, which is related to the sum of the derivative of the energy with respect to the finite range and the averaged kinetic energy of opposite spin pairs. By comparing the $1/k^4$ term and the $1/k^6$ correction in the momentum distribution to provided Quantum Monte Carlo (QMC) data, we show that including the $1/k^6$ part offers marked improvements. Our field theoretical approach allows for a clear understanding of the role of the scattering length and finite effective range in the universal relations and the momentum distribution.

PACS numbers: 03.75.Ss, 31.15.-p, 31.15.xp, 34.50.-s, 67.85.Lm

I. INTRODUCTION

Strongly interacting systems of ultracold two-component fermions have been studied using various techniques for many years. In nuclear physics this system is of interest due to its simplicity and similarity to a gas of ultracold neutrons. In atomic physics, this system is of interest because of its transition from a Bose-Einstein condensate (BEC) at small positive scattering lengths to a system that displays BCS superfluidity at small negative scattering lengths. Specifically, the case called the *unitary limit*, in which the two-body scattering length a is taken to infinity, received a lot of attention from experimentalists and theorists alike [1]. In this limit the zero-range model can be used to describe systems with large scattering length. In this model, the range of the atom-atom interaction is taken to zero while the binding energy is kept constant by adjustment of the coupling strength.

Universal relations, which are independent of the structure of the particles and the state of the system, were derived in the zero range limit for these systems by Shina Tan in 2005 [2–4]. These relations contain the so-called *contact* that can be defined as the asymptote of the $1/k^4$ large momentum tail of the momentum distribution. The contact is a state dependent quantity and will therefore depend on quantities such as the scattering length, temperature, or density of the system.

Tan’s contact and the related universal relations can be derived by applying the operator product expansion

(OPE) [5–7], which is the quantum field theoretical short-distance expansion of a nonlocal operator. In Ref. [8], it was shown that this tool can be used to derive Tan’s universal relations and that the contact is related to the leading two-body interaction term in the OPE. The OPE has since then been used not only to derive additional universal relations for the two-component Fermi gas, but it has also been applied to novel systems such as the unitary Bose gas [9–20] (for a discussion of other approaches that have been used to derive universal relations see Ref. [21] and the references therein).

In this manuscript, we derive improved universal relations which include the finite effective range of the two-body interaction. Just as the contact was identified as playing an important role in the zero-range limit, we identify two quantities that appear in universal relations valid beyond the zero-range limit. One of them, which we call the *derivative contact*, is a measure of the sensitivity of the energy of the system to the effective range. The other measures the averaged kinetic energy of opposite spin pairs at zero relative distance. Some of these relations were already derived using a quantum mechanical framework by Castin and Werner in Ref. [22]. Here we will use the OPE framework and an effective field theory (EFT) to derive additional finite-range universal relations. In the EFT approach an existing separation of scales is turned into an expansion parameter for a systematic low-energy perturbative expansion. In our case this expansion parameter is the ratio ℓ/a , where ℓ denotes the range of the atom-atom interaction. This approach is very powerful since it makes no assumptions regarding the microscopic interaction responsible for the large scattering length and is therefore completely model-independent.

First, we review the theory that is used to describe particles interacting through a short-range interaction in

*Electronic address: semmons@vols.utk.edu

†Electronic address: kang1@lanl.gov

‡Electronic address: lplatter@utk.edu

Sec. II. We present the renormalization of the theory up to both Leading Order (LO) and Next-to-Leading Order (NLO) in the EFT expansion. Renormalization eliminates divergences which arise in the field theoretical calculations and leaves us with physical, finite results. After presenting the EFT model we use, we move directly to the results and leave the detailed calculations of those results for later. Thus, Sec. III shows universal relations with effective range corrections, including a subleading, in the OPE expansion, tail of the momentum distribution and corrections to the energy, adiabatic, and pressure relations and to the virial theorem. Section IV gives a numerical comparison between the contact and the derivative contact and shows the OPE result in comparison to Quantum Monte Carlo (QMC) data. Lastly, Sec. V contains the many details of the OPE calculations which lead to the results already presented in Sec. III. The renormalized two-body operators in the OPE form the contact and derivative contact operators which are in the universal relations.

II. EFFECTIVE FIELD THEORY

For an interaction with finite range, ℓ , the two-body t-matrix can be written as

$$t(k) = \frac{4\pi}{m} \frac{1}{k \cot \delta_0 - ik}, \quad (1)$$

where m denotes the particle mass, k is the relative momentum between the two particles, and δ_0 is the scattering phaseshift. At sufficiently low energies, we can expand $k \cot \delta_0$ using the effective range expansion

$$k \cot \delta_0 = -\frac{1}{a} + \frac{r_s}{2} k^2 + \dots, \quad (2)$$

where a is the S -wave scattering length, and r_s is the S -wave effective range. For $k\ell \ll 1$, the short-range details of the interaction are not resolved and such systems can therefore be described with an EFT that employs only contact interactions.

The EFT Lagrangian for particles interacting through contact interactions can be written as

$$\mathcal{L} = \mathcal{L}_0 + \mathcal{L}_1 + \dots, \quad (3)$$

where $\mathcal{L}_{0,1}$ are leading order (LO) and next-to-leading order (NLO) in r_s Lagrangians and the dots denote operators with more derivatives and/or fields that contribute to higher orders in the EFT expansion. The LO and NLO Lagrangians are given by

$$\mathcal{L}_0 = \sum_{\sigma=1,2} \psi_{\sigma}^{\dagger} \left(i\partial_t + \frac{\nabla^2}{2m} \right) \psi_{\sigma} - \frac{\lambda_0}{m} \psi_1^{\dagger} \psi_2^{\dagger} \psi_2 \psi_1 \quad (4)$$

$$\mathcal{L}_1 = \frac{\rho_0}{4} \left(\psi_1^{\dagger} \psi_2^{\dagger} \psi_2 \overleftrightarrow{\nabla}^2 \psi_1 + \text{h.c.} \right) + \delta\mathcal{L}_1, \quad (5)$$

$$\delta\mathcal{L}_1 = -\frac{\delta\lambda_0}{m} \psi_1^{\dagger} \psi_2^{\dagger} \psi_2 \psi_1. \quad (6)$$



FIG. 1: Scattering amplitude at leading order.

Note that we have set $\hbar = 1$. When considered by itself, Lagrangian \mathcal{L}_0 is also known as the zero-range model, and we will show below how the bare coupling λ_0 is related to the scattering length a through renormalization. \mathcal{L}_1 consists of the effective range term, proportional to ρ_0 , and $\delta\mathcal{L}_1$, which is present to subtract a divergence which arises in the calculation of the scattering amplitude with this Lagrangian. Below we will regularize all integrals with a sharp UV cutoff. We will renormalize the LO and NLO expressions below, calculating the coupling constants λ_0 , ρ_0 , and counter term $\delta\lambda_0$ of the theory, to reproduce the t-matrix in each case.

A. LO amplitude

At LO in r_s , the λ_0 vertex has to be iterated to all orders in order to reproduce the non-perturbative properties of the large scattering length limit [23, 24]. The diagrams contributing to the two-body scattering amplitude form the integral equation shown in Fig. 1, that is equivalent to the Lippmann-Schwinger (LS) equation,

$$i\mathcal{A}_{LO}(E) = -i\frac{\lambda_0}{m} - i\frac{\lambda_0}{m} \mathcal{I}_0(E, \Lambda) i\mathcal{A}_{LO}(E), \quad (7)$$

where E denotes total energy of the two-body system. On the mass shell $E = k^2/m$. The function $\mathcal{I}_0(E, \Lambda)$ in Eq. (7) is given in Eq. (A2) in Appendix A. It is the loop integral shown in Fig. 1 and depends on the energy E and the ultraviolet (UV) cutoff Λ that is imposed on the integral.

The low-energy constant λ_0 is a function of the cutoff and its form is determined by requiring that Eq. (7) reproduces the two-body t-matrix in Eq. (1) in the limit $r_s \rightarrow 0$. We can therefore write λ_0 explicitly as a function of the cutoff Λ and the scattering length a

$$\lambda_0 = \frac{4\pi a}{1 - 2a\Lambda/\pi}. \quad (8)$$

B. NLO amplitude

In this subsection we present the renormalization of the EFT including short-range interactions up to NLO. The renormalization to this order using dimensional regularization with power divergence subtraction (PDS) was already discussed in [23]. Since we are using an explicit momentum space cutoff, we have to introduce an additional subtraction terms as we will discuss below.

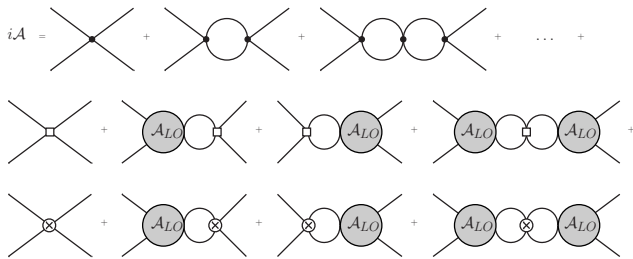


FIG. 2: Scattering amplitude up to NLO. The solid dot denotes a λ_0 vertex, the square represents the ρ_0 vertex, and the symbol crossed circles represent the counterterm vertex, $\delta\lambda_0$.

The expansion of the two-body t-matrix in Eq. (1) in r_s can be written as

$$t(k) = \frac{4\pi}{m} \frac{1}{-\frac{1}{a} - ik} \left(1 - \frac{r_s k^2}{-\frac{1}{a} - ik} \right), \quad (9)$$

where the first term is LO and second term is its NLO correction. We would like to reproduce the second term by calculating corrections to the two-body amplitude perturbatively due to \mathcal{L}_1 .

In Fig. 2, we show the scattering amplitude up to NLO. The second row contains the sum of the diagrams with exactly one insertion of the ρ_0 vertex. The third row shows the diagrams that contain exactly one insertion of the $\delta\lambda_0$ vertex. The factors ρ_0 and $\delta\lambda_0$ are inserted only once because, as we will see below, they are proportional to r_s , which we only want one factor of inserted to perform the calculation at NLO in the effective range. In addition to these two contributions, we have to consider a contribution that arises from resumming the λ_0 vertex as a result of using a finite cutoff regularization scheme, which introduces a correction on the order of $1/\Lambda$.

The sum of these three contributions is given by

$$i\mathcal{A}_{\text{NLO}} = -i\mathcal{A}_{\text{LO}}^2 \frac{mk^2}{2\pi^2\Lambda} - i2\rho_0 \frac{m\mathcal{A}_{\text{LO}}^2}{\lambda_0} \left(\frac{mk^2}{\lambda_0} - \frac{m\Lambda^3}{6\pi^2} \right) - i\frac{\delta\lambda_0}{m} \left(\frac{m\mathcal{A}_{\text{LO}}}{\lambda_0} \right)^2. \quad (10)$$

Each term gives the contribution from each of the three rows in Fig. 2 at NLO. In the first term, we keep only the NLO contribution proportional to $\frac{k^2}{\Lambda}$ after summing over all diagrams in the first row of the figure. The second contribution is the sum of diagrams for the effective range vertex, and it contains a Λ^3 divergence. Requiring that the third term, proportional to $\delta\lambda_0$, subtracts the $\mathcal{O}(\Lambda^3)$ divergence and then comparing Eq. (10) to the NLO term in Eq. (9), ρ_0 and $\delta\lambda_0$ are determined to be

$$\rho_0 = \frac{\lambda_0^2}{16\pi m} \left(r_s - \frac{4}{\pi\Lambda} \right), \quad (11)$$

$$\delta\lambda_0 = \frac{(\lambda_0\Lambda)^3}{48\pi^3} \left(r_s - \frac{4}{\pi\Lambda} \right). \quad (12)$$

III. UNIVERSAL RELATIONS AT NEXT-TO-LEADING ORDER

In addition to the given field theoretical framework, we use the OPE to calculate the momentum distribution and find the contact, C , the derivative contact, D , and the operator C' that measures the mean kinetic energy of opposite spin pairs in terms of renormalized field theoretical operators. Then we express the other relations in terms of the operators associated with these parameters. However, we leave the details of this to Sec. V and directly present the results here. We give the $1/k^6$ correction to the $1/k^4$ tail of momentum distribution and effective range corrections to the energy relation, adiabatic relation, pressure relation, and to the virial theorem for a harmonic potential.

By using the OPE, we find that the momentum distribution of atoms in a spin state σ is given by

$$\rho_\sigma(k) \rightarrow \frac{C}{k^4} + \frac{C' + D}{k^6} + \mathcal{O}\left(\frac{1}{k^8}\right), \quad (13)$$

where C is the well-known contact, which is the asymptote of the scaled momentum distribution shown in Fig. 4 and a measure of the sensitivity of the system to the scattering length. We call D the derivative contact because it is associated with the second derivative of the contact operator in \mathcal{L}_0 , and it is a measure of the sensitivity of the system to the finite effective range, r_s . C' is associated with the averaged pair kinetic energy in the system. In the two-body system $C' = CK^2/2$, where K is the center of mass momentum. In the absence of a known value for C' , we do not include it in Fig. 4 below. However, a value could be obtained from the $1/k^6$ tail of improved QMC simulation data. Note that Eq. (13) is valid in the limit of zero effective range and that the form remains the same after taking the effective range correction into account because the correction is contained in C , C' , and D . The derivation of Eq. (13) is given separately in Sec. V, where we also show that the contact C and derivative contact D are the expectation values $\langle \int d^3\mathbf{R} \mathcal{O}_C \rangle$ and $\langle \int d^3\mathbf{R} \mathcal{O}_D \rangle$, respectively. \mathcal{O}_C is proportional to the contact term in \mathcal{L}_0 , with coupling constant λ_0 , in the Lagrangian, and the operator \mathcal{O}_D is related to \mathcal{L}_1 . Similarly, near p - or d -wave resonances [25, 26], the $1/k^4$ term in the tail of the momentum distribution receives contributions with interpretations similar to C' and D .

Next, the energy relation rewrites the sum of kinetic and interaction energies, each separately sensitive to UV behavior in this field theoretical framework, in terms of pieces which are individually finite.

$$\langle H \rangle = \frac{C}{4\pi ma} + r_s \frac{D}{16\pi m} + \langle T^{(\text{sub})} \rangle, \quad (14)$$

where $\langle H \rangle$ is the expectation value of the Hamiltonian for a generic mixture of eigenstates, and $T^{(\text{sub})}$ is the subtracted (renormalized) kinetic energy defined here in Eq. (15), which is calculated using Eq. (66) found at the

end of Sec. V.

$$\begin{aligned} & \langle T^{(\text{sub})} \rangle \\ &= \sum_{\sigma} \int_0^{\infty} \frac{dk}{4\pi^2 m} \left[k^4 \rho_{\sigma}(k) - C - \frac{\theta(k - k_0)}{k^2} (C' + D) + \dots \right] \\ &+ \frac{C' + D}{2\pi^2 m k_0} - r_s \frac{C' + 3D}{16\pi m}. \end{aligned} \quad (15)$$

To arrive at this, the kinetic energy operator \mathcal{T} defined in Sec. V was rewritten in terms of the renormalized operator in Eq. (43). Then this was replaced by the momentum distribution $\rho_{\sigma}(k)$ using the OPE result given in Eq. (59). The lower limit $k > k_0$ was imposed to prevent an IR divergence, and the second to last term was added to remove sensitivity to the IR cutoff. The derivation of Eq. (14) is given after the derivation of the momentum distribution at the end of Sec. V. While the energy relation holds for a generic mixture of states, the relations that follow in the remainder of this section are for a pure eigenstate. In the case of a generic mixture they approximately hold, and only so long as the off diagonal terms are negligible as discussed in [2–4].

The adiabatic relation [3] is defined as the change in the energy of the system due to an adiabatic change of a so that the energy eigenstate of the system is not disturbed. A similar adiabatic relation for the effective range r_s can be obtained by taking the derivative with respect to r_s . Taking the derivative of the energy of the system with respect to a gives

$$\frac{dE}{da} = \left\langle \frac{dH}{da} \right\rangle = \frac{C}{4\pi m a^2}, \quad (16)$$

where, for the first equality, we used the Feynman-Hellmann theorem. Then, for the second equality we obtain $dH/da = \int d^3\mathbf{R} \mathcal{O}_C / (4\pi m a^2) + O(1/\Lambda^2)$ by using $d\lambda_0/da = \lambda_0^2 / (4\pi a^2)$ and $d\rho_0/da = \frac{\lambda_0}{2\pi a^2} \rho_0$. Note that Eq. (16) remains the same as it was in the zero-range limit, $r_s \rightarrow 0$, in Ref. [4], and the effective range correction is contained in the expectation value C .

Taking the derivative of the energy respect to r_s , with a held fixed, gives

$$\frac{dE}{dr_s} = \left\langle \frac{dH}{dr_s} \right\rangle = \frac{D}{16\pi m}, \quad (17)$$

where we again used the Feynman-Hellmann theorem in the first equality and then obtained $dH/dr_s = \mathcal{O}_D / (16\pi m) + O(\rho_0)$ by using $d\rho_0/dr_s = \lambda_0^2 / (16\pi m)$ and $da/dr_s = d\lambda_0/dr_s = d\Lambda/dr_s = 0$. Any terms proportional to ρ_0 should be dropped because they are higher order than NLO when in H . This means that D is independent of r_s at NLO in r_s . In other words, dE/dr_s is well behaved as $r_s \rightarrow 0$, as discussed in [22, 27, 28].

Next, we derive the effective range corrections to the pressure relation [4] and the virial theorem [29]. For a homogeneous gas, the energy scales linearly with the volume of the system. Thus, the energy density is a function of volume-independent variables. For example, the

Helmholtz free energy density \mathcal{F} depends only on intensive thermodynamic quantities such as temperature, T , chemical potential, μ_{σ} , and interaction parameters such as a and r_s . Dimensional analysis implies the following equality

$$\left[T \frac{\partial}{\partial T} + \mu_{\sigma} \frac{\partial}{\partial \mu_{\sigma}} - \frac{a}{2} \frac{\partial}{\partial a} - \frac{r_s}{2} \frac{\partial}{\partial r_s} \right] \mathcal{F} = \frac{5}{2} \mathcal{F}, \quad (18)$$

where the LHS is the sum of the logarithmic derivative with respect to each individual parameter of the system multiplied by its dimension, and it reduces to the free energy density multiplied by its energy dimension, $5/2$. By using the definition $\mathcal{F} = \mathcal{E} - Ts$, where s is the entropy density, and the relation $\mathcal{F} = -P + \mu_{\sigma} n_{\sigma}$, where μ_{σ} is the chemical potential, for a homogeneous system and eliminating Ts and $\mu_{\sigma} n_{\sigma}$ in favor of \mathcal{E} and P , we obtain the pressure relation as

$$P = \frac{2}{3} \mathcal{E} + \frac{\mathcal{C}}{12\pi m a} + r_s \frac{\mathcal{D}}{48\pi m}, \quad (19)$$

where \mathcal{E} , \mathcal{C} , and \mathcal{D} are E , C , and D divided by volume of the system.

For a gas trapped in a harmonic potential, $V(\mathbf{R})$, with frequency ω , we see from dimensional analysis that the energy obeys the relation

$$\left[\sum_i \omega_i \frac{\partial}{\partial \omega_i} - \frac{a}{2} \frac{\partial}{\partial a} - \frac{r_s}{2} \frac{\partial}{\partial r_s} \right] E = E. \quad (20)$$

By using $\sum_i \omega_i \partial V(\mathbf{R}) / \partial \omega_i = 2V(\mathbf{R})$ and Eqs. (16) and (17) we obtain the virial theorem for a trapped atomic gas:

$$E = 2V - \frac{C}{8\pi m a} - r_s \frac{D}{32\pi m}, \quad (21)$$

where V is an average of the harmonic potential for the system.

The subleading $1/k^6$ tail in the OPE expansion of the momentum distribution and its relation to energy in Eqs. (13) and (17) were first derived in [22] by analyzing the behavior of the many-body wave function for systems of two-component fermions with a large two-body scattering length a . We reproduce the same results by using the OPE for two-body states.

IV. GROUND STATE RESULTS FOR A HOMOGENEOUS GAS

In this section we extract the numerical value of the derivative contact D from the recent QMC calculations and compare it to the value of the contact, C , in the zero range limit. We also plot the momentum distribution in comparison to QMC simulation data.

Near the unitary limit, the energy density of a balanced homogeneous Fermi gas in its ground state can be

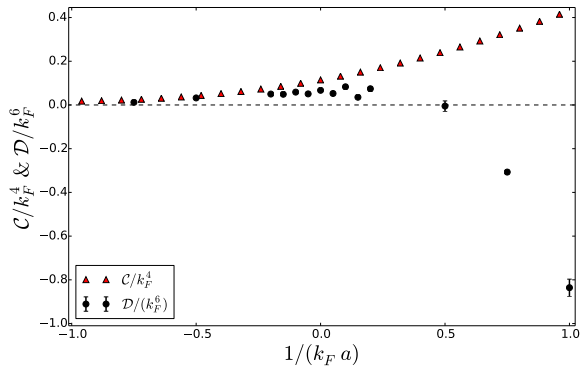


FIG. 3: (color online) Dimensionless contact density \mathcal{C}/k_F^4 , represented by the triangles on the graph, and the derivative contact density \mathcal{D}/k_F^6 as function of $1/(k_F a)$ at zero temperature from QMC simulation in [27, 28].

expressed as

$$\mathcal{E} = \left(\xi - \frac{\zeta}{k_F a} + S k_F r_s + \dots \right) \mathcal{E}_F, \quad (22)$$

where $\mathcal{E}_F = \frac{1}{10\pi^2} k_F^5/m$ is the Fermi energy density, $k_F = (3\pi^2 n)^{1/3}$ is the Fermi momentum, and n is the total number density. ξ is the Bertsch parameter; ζ and S are slope constants with respect to the $1/(k_F a)$ and $k_F r_s$ axes, respectively, in the unitary limit. Away from unitarity they are not constant, but the energy density still contains an effective range correction proportional to $k_F r_s$. Also, the slope S becomes a function of $k_F a$.

The contact density \mathcal{C} of the Fermi gas can be obtained in various limits using the expressions for the energy in those limits, such as that in the unitary limit given by Eq. (22), and using Eq. (16) to arrive at Eqs. (23), (24), and (25).

$$\mathcal{C}/k_F^4 \rightarrow \frac{4}{9\pi^2} (k_F a)^2, \quad a \rightarrow 0^- \text{ (BCS limit)} \quad (23)$$

$$\rightarrow \frac{2\zeta}{5\pi}, \quad a \rightarrow \pm \infty \text{ (unitary limit)} \quad (24)$$

$$\rightarrow \frac{4}{3\pi} (k_F a)^{-1}, \quad a \rightarrow 0^+ \text{ (BEC limit)} \quad (25)$$

where ζ is the constant in Eq. (22) determined from experiment or calculated by various theoretical methods. The energy density in the BCS and BEC limits are given in Ref. [21]. The dimensionless contact density \mathcal{C}/k_F^4 is parametrically suppressed by $(k_F a)^2$ in the BCS limit and is parametrically enhanced by $1/(k_F a)$ in the BEC limit, and it increases as one goes through unitarity from the BCS to the BEC limit.

The contact has been determined from many observables by various experimental groups. The contact across the BCS-BEC crossover was first determined from photo association [30, 31]. Precise values in the unitary limit were obtained: $\zeta = 0.93(5)$ from a thermodynamic mea-

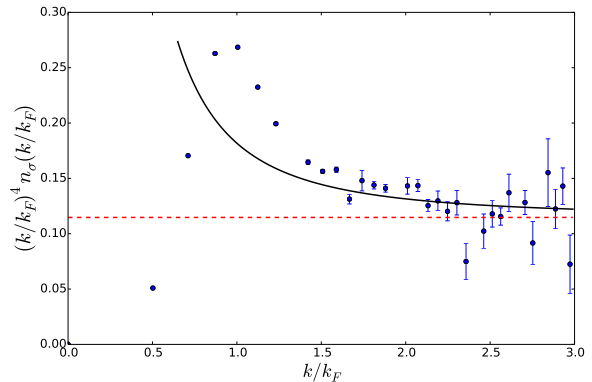


FIG. 4: (color online) Scaled momentum distribution near unitarity, $(k/k_F)^4 n_\sigma(k/k_F)$, where σ indicates either of two spin states, as a function of k/k_F in comparison to QMC result [28]. The dashed horizontal line is \mathcal{C}/k_F^4 . The solid line is $\mathcal{C}/k_F^4 + \mathcal{D}/(k_F^4 k^2)$. We use the values near unitarity of $\mathcal{C}/k_F^4 = 0.115$ and $\mathcal{D}/k_F^6 = 0.061$.

surement [32] and $\zeta = 0.91(4)$ from the static structure factor [33]. The temperature dependence was determined from the structure factor using Bragg spectroscopy [33, 34] and also from RF spectroscopy [35]. Various universal relations have been verified by testing the consistency of numerical values of the contact determined from different observables and properties of the system such as the momentum distribution, the RF line shape, photoemission spectra, the adiabatic theorem, and the virial theorem [36].

The contact has been calculated not only using QMC [37–42], but also with other methods[43–45]. Currently, the most accurate theoretical value is $\zeta = 0.901(3)$ given in [46]. Near unitarity this gives a value of $\mathcal{C}/k_F^4 \approx 0.115$.

Additionally, the slope S in Eq. (22) has been calculated in [27, 28], and the density of the derivative contact for the ground state is

$$\mathcal{D} = \frac{8k_F^6}{5\pi} S(k_F a). \quad (26)$$

Some of the asymptotic behavior of the derivative contact density is given by

$$\begin{aligned} \mathcal{D}/k_F^6 &\rightarrow \frac{8S}{5\pi}, & a \rightarrow \pm \infty \text{ (unitary limit)} \\ &\rightarrow -0.9(1) (k_F a)^{-3}, & a \rightarrow 0^+ \text{ (BEC limit)} \end{aligned} \quad (27)$$

where $S = 0.12(1)$ was obtained in [28]. This gives a value of $\mathcal{D}/k_F^6 = 0.061$ in the unitary limit. Equation (27) can be derived using Eq. (22) and the relation between \mathcal{D} and dE/dr_s found in Eq. (17). We calculated the result, namely $\mathcal{D}/k_F^6 \rightarrow -0.9(1) (k_F a)^{-3}$, in the BEC limit, $1/k_F a > 0$, by fitting \mathcal{D} to the QMC data for S [28] shown in Fig. 3 (note that this figure contains the data rescaled with the prefactor given in Eq. (26)). The dimer binding energy $E_{\text{dimer}} = 1/(ma^2)[1 + r_s/a + \dots]$ gives

the derivative contact for the dimer as $D_{\text{dimer}} = 16\pi/a^3$, which is consistent with the power law in the BEC limit. A power law in the BCS limit is not known.

Figure 3 shows results for the scaled contact density \mathcal{C}/k_F^4 and derivative contact density \mathcal{D}/k_F^6 as a function of $1/(k_F a)$. In the unitary limit \mathcal{C} is about twice as large as \mathcal{D} . In the BEC limit the magnitude of \mathcal{D} increases faster than that of \mathcal{C} , and this follows from the fact that the effective range correction is more important in this limit as the approximation of universal physics worsens. Fig. 4 shows a scaled momentum distribution in unitary limit. The OPE results in Eq. (13) describe the QMC data [28] well for large $k > 1.5k_F$. However, we note again that we did not include the unknown C' contribution in this analysis.

V. OPERATOR PRODUCT EXPANSION AND RELATED CALCULATIONS

In what follows we describe the expansion of the nonlocal operator for the momentum distribution in the large k , or short-distance, limit, that we use in the derivation of the above universal relations. With the OPE we derive expressions for the contact and derivative contact in terms of field theoretical operators. We then express the Hamiltonian in terms of those operators. The OPE, invented independently by Ken Wilson [5], Leo Kadanoff [6], and Alexander Polyakov [7] in 1969, is a short-distance expansion of a nonlocal operator into a series of local operators multiplied with short-distance coefficients, or Wilson coefficients, that are functions of the relative separation \mathbf{r} :

$$\mathcal{O}_A\left(\mathbf{R} - \frac{\mathbf{r}}{2}\right)\mathcal{O}_B\left(\mathbf{R} + \frac{\mathbf{r}}{2}\right) = \sum_n W_n(\mathbf{r})\mathcal{O}_n(\mathbf{R}), \quad (28)$$

where W_n is the Wilson coefficient of the local operator \mathcal{O}_n . In this paper we consider the nonlocal one-body density operator $\psi_\sigma^\dagger(\mathbf{R} - \mathbf{r}/2)\psi_\sigma(\mathbf{R} + \mathbf{r}/2)$, which is a coordinate space representation of the momentum distribution and gives the momentum space distribution $\rho_\sigma(k)$ after a Fourier transform.

The operators on the RHS in Eq. (28) can be constructed from the fields of the EFT and their gradients. The field ψ_σ has dimension $\Delta = 3/2$ in our EFT expansion, the Galilean invariant derivative

$$\overleftrightarrow{\partial}_i = \overrightarrow{\partial}_i - \overleftarrow{\partial}_i \quad (29)$$

has $\Delta = 1$, and the time derivative ∂_t has $\Delta = 2$. Here, we list the relevant operators up to dimension $\Delta = 6$.

Δ	$\mathcal{O}_{1,\Delta}$	$\mathcal{O}_{2,\Delta}$
3	$\psi_\sigma^\dagger \psi_\sigma$	
4	$\psi_\sigma^\dagger \overleftrightarrow{\partial}_i \psi_\sigma$	$\psi_1^\dagger \psi_2^\dagger \psi_2 \psi_1$
5	$\psi_\sigma^\dagger \overleftrightarrow{\partial}_i \overleftrightarrow{\partial}_j \psi_\sigma$	$\psi_1^\dagger \psi_2^\dagger \psi_2 \overleftrightarrow{\partial}_i \psi_1 + h.c.$
6	$\psi_\sigma^\dagger \overleftrightarrow{\partial}_i \overleftrightarrow{\partial}_j \overleftrightarrow{\partial}_k \psi_\sigma$	$\psi_1^\dagger \psi_2^\dagger \psi_2 \overleftrightarrow{\partial}_i \overleftrightarrow{\partial}_j \psi_1 + h.c.$

(30)

A unit operator is omitted since the momentum distribution for the vacuum is zero while the unit operator vacuum expectation value is nonzero, and the operator with time derivative ∂_t is excluded because we can always eliminate it in favor of momentum-dependent operators by using the equations of motion obtained from Eqs. (4) and (5) [11]. In the first column of the operator list the number in each row represents the dimension of operators in that row. The second and the third column list the one-body and two-body operators as indicated in the subscript of $\mathcal{O}_{1,\Delta}$ and $\mathcal{O}_{2,\Delta}$. It is known [8] that the dimension of $\psi_1^\dagger \psi_2^\dagger \psi_2 \psi_1$ is lowered down to $\Delta = 4$ from $\Delta = 6$ by the strong interaction, and we find that this is true for the operator $\psi_1^\dagger \psi_2^\dagger \psi_2 \overleftrightarrow{\partial}_i \overleftrightarrow{\partial}_j \psi_1$ so that it has $\Delta = 6$ rather than 8.

Rewriting Eq. (28) for our problem we have

$$\begin{aligned} & \psi_\sigma^\dagger(\mathbf{R} - \mathbf{r}/2)\psi_\sigma(\mathbf{R} + \mathbf{r}/2) \\ &= \sum_{\Delta} (W_{1,\Delta}(\mathbf{r})\mathcal{O}_{1,\Delta}(\mathbf{R}) + W_{2,\Delta}(\mathbf{r})\mathcal{O}_{2,\Delta}(\mathbf{R}) + \dots), \end{aligned} \quad (31)$$

where the first index n of each $W_{n,\Delta}$ indicates whether the coefficient is for a one- or two-body operator, and the second index Δ gives the scaling dimension of that operator. We determine the Wilson coefficients of one- and two-body operators up to $\Delta = 6$.

Before we calculate the matrix elements of the operators shown above, we discuss briefly the off-shell scattering amplitude, whose knowledge is required for the derivation of our Wilson coefficients. In the renormalization of the EFT in Sec. II, we considered the on-shell amplitude depending on the relative momentum k , with $k^2 = mE$, but we use the off-shell amplitude during operator matching since its explicit momentum dependence contributes to the loop integral results in our calculations. In general, the off-shell amplitude with incoming momenta $(E/2, \pm\mathbf{p})$ and outgoing momenta $(E/2, \pm\mathbf{k})$ should be a function of three variables: E , \mathbf{p} , and \mathbf{k} . However it is known that the LO amplitude, $\mathcal{A}_{\text{LO}}(E)$, depends solely on the total energy and not on external momenta. This simplifies the calculation of a loop diagram involving $\mathcal{A}_{\text{LO}}(E)$, such as the last graph in Fig. 1, by factorizing it into a product of the amplitude and the loop integral as shown in the last term of Eq. (7). However, this is not true at NLO. Expanding the off-shell amplitude in powers of $1/\Lambda$ we obtain

$$\begin{aligned} \mathcal{A}_{\text{LO}} - \mathcal{A}_{\text{LO}}^2 \frac{m(mE)}{2\pi^2\Lambda} - \mathcal{A}_{\text{LO}}^2 \frac{2m^2\rho_0 mE}{\lambda_0^2} \\ + \mathcal{A}_{\text{LO}} \frac{m\rho_0}{\lambda_0} (\mathbf{p}^2 + \mathbf{k}^2 - 2mE) + \dots, \end{aligned} \quad (32)$$

where the first term, the LO amplitude, is proportional to $1/E$ and the next two terms are NLO in $1/\Lambda$ and reduce to Eq. (10) in the on-shell limit. The last term, proportional to \mathbf{p}^2/Λ^2 , and terms beyond this are power suppressed. Here, we count the size of parameters as



FIG. 5: Diagrams for the operator $\langle \psi_\sigma^\dagger(\mathbf{R}-\mathbf{r}/2)\psi_\sigma(\mathbf{R}+\mathbf{r}/2) \rangle$ for the 2 atom scattering state. The empty dots imply locations $\pm\mathbf{r}/2$ where an atom is annihilated and created at an equal time.

follows: $a^{-1}, \mathbf{p}, \mathbf{k}, \sqrt{mE}$ are of the same size and much smaller than Λ , while $\lambda_0 \sim 1/\Lambda$ and $\rho_0 \sim 1/\Lambda^3$. The terms of order $1/\Lambda^2$ and higher can be dropped when the final goal is to compute the amplitude at NLO, and \mathcal{A} then depends only on E , becoming $\mathcal{A}_{\text{NLO}}(E)$. But, in the calculation of matrix elements, the term proportional to $\mathbf{p}^2 + \mathbf{k}^2$ contributes factors of the loop momentum in the loop diagrams involving the amplitude and can lead to a UV divergence. Therefore, terms of $\mathcal{O}(1/\Lambda^2)$ can only be dropped at the end of the calculation.

At the end of calculations we keep terms only up to NLO in $(1/\Lambda)$ and renormalize the operators either by multiplying by a renormalization factor or by adding different operators as counterterms to subtract the divergences and Λ -dependence. We rewrite the full off-shell amplitude $\mathcal{A}(E, \mathbf{p}, \mathbf{k})$ in terms of an amplitude $\mathcal{A}_\lambda(E)$ that contains only diagrams that contain the λ_0 -coupling constant and amplitudes $\mathcal{A}_\rho(E)$ and $\mathcal{A}_{\rho'}(E)$ that contain one insertion of the ρ_0 -coupling constant but scale as $1/\Lambda$ and $1/\Lambda^2$, respectively. In these amplitudes, all power suppressed terms $(\sqrt{mE}/\Lambda)^n$ in the loop integral $\mathcal{I}_0(E, \Lambda)$ are retained. The amplitude is given as

$$\begin{aligned} \mathcal{A}(E, \mathbf{p}, \mathbf{k}) &= \mathcal{A}(E) + (\mathbf{p}^2 + \mathbf{k}^2 - 2mE)\mathcal{A}_{\rho'}(E), \\ \mathcal{A}(E) &= \mathcal{A}_\lambda(E) + \mathcal{A}_\rho(E), \\ \mathcal{A}_\lambda &= -\frac{1}{m/\lambda_0 + i\mathcal{I}_0(E, \Lambda)}, \\ \mathcal{A}_\rho &= -\frac{2\rho_0 m^2}{\lambda_0^2} mE \mathcal{A}_\lambda^2, \\ \mathcal{A}_{\rho'} &= \frac{\rho_0 m}{\lambda_0} \mathcal{A}_\lambda, \end{aligned} \quad (33)$$

where $\mathcal{I}_0(E, \Lambda)$ is given in the Appendix in Eq. (A2). Also, the amplitude \mathcal{A}_λ still satisfies the LS equation in Eq. (7) when \mathcal{A}_{LO} is replaced by \mathcal{A}_λ .

$$\mathcal{A}_\lambda = -\lambda_0/m(1 + \mathcal{I}_0 i\mathcal{A}_\lambda). \quad (34)$$

Figure 5 shows diagrams contributing to the matrix element for the two-atom scattering state with incoming momenta $(p_0, \pm\mathbf{p})$, with outgoing momenta $(k_0, \pm\mathbf{k})$, and with total energy $E = 2p_0 = 2k_0$. We generalize to a system with non-zero center-of-mass momentum later in this section. The matrix element of the nonlocal operator is given by

$$\begin{aligned} &\langle \psi_\sigma^\dagger(\mathbf{R} - \frac{\mathbf{r}}{2})\psi_\sigma(\mathbf{R} + \frac{\mathbf{r}}{2}) \rangle \\ &= \delta_{\mathbf{p}\mathbf{k}} e^{i\mathbf{p}\cdot\mathbf{r}} + \left[\frac{ie^{i\mathbf{p}\cdot\mathbf{r}}}{p_0 - \frac{\mathbf{p}^2}{2m}} i\mathcal{A}(E) + (p \rightarrow k) \right] - \mathcal{I}_{\rho,0} \mathcal{A}^2(E) \\ &\quad - 2\left[\left(\frac{\mathbf{p}^2 + \mathbf{k}^2}{2} - 2mE \right) \mathcal{I}_{\rho,0} + \mathcal{I}_{\rho,2} \right] \mathcal{A}_\lambda \mathcal{A}_{\rho'}, \end{aligned} \quad (35)$$

where we use the shorthand notation $\delta_{\mathbf{p}\mathbf{k}} = (2\pi)^3 \delta^{(3)}(\mathbf{p} - \mathbf{k})$, and the one-loop integral $\mathcal{I}_{\rho,2n}$ is given in the Appendix in Eq. (A10).

By inserting $\mathcal{I}_{\rho,0}$ and $\mathcal{I}_{\rho,2}$ from Eq. (A10) into Eq. (35) and expanding in powers of r up to r^3 , we obtain

$$\begin{aligned} \langle \psi_\sigma^\dagger(\mathbf{R} - \frac{\mathbf{r}}{2})\psi_\sigma(\mathbf{R} + \frac{\mathbf{r}}{2}) \rangle &= \delta_{\mathbf{p}\mathbf{k}} - \left[\frac{\mathcal{A}(E)}{p_0 - \frac{\mathbf{p}^2}{2m}} + (p \rightarrow k) \right] + \frac{i\mathcal{A}^2(E)m^2}{8\pi\sqrt{mE}} \\ &\quad + ir_i p_i \delta_{\mathbf{p}\mathbf{k}} - ir_i \left[\frac{p_i \mathcal{A}(E)}{p_0 - \frac{\mathbf{p}^2}{2m}} + (p \rightarrow k) \right] - r \frac{\mathcal{A}^2(E)m^2}{8\pi} \\ &\quad - r_i r_j \frac{p_i p_j}{2} \delta_{\mathbf{p}\mathbf{k}} + \frac{r_i r_j}{2} \left[\frac{p_i p_j \mathcal{A}(E)}{p_0 - \frac{\mathbf{p}^2}{2m}} + (p \rightarrow k) \right] - ir^2 \frac{\mathcal{A}^2(E)m^2\sqrt{mE}}{16\pi} \\ &\quad - ir_i r_j r_k \frac{p_i p_j p_k}{6} \delta_{\mathbf{p}\mathbf{k}} + i \frac{r_i r_j r_k}{6} \left[\frac{p_i p_j p_k \mathcal{A}(E)}{p_0 - \frac{\mathbf{p}^2}{2m}} + (p \rightarrow k) \right] + r^3 \frac{\mathcal{A}^2(E)m^3 E}{48\pi} \\ &\quad + \mathcal{O}(r^4), \end{aligned} \quad (36)$$

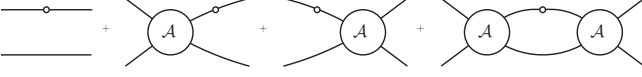


FIG. 6: Diagrams for one-body operator. Empty dots imply an insertion of the one-body operator given in Eq. (30) and $\mathcal{A}(E, \mathbf{p}, \mathbf{k})$ represents the off-shell amplitude in Eq. (33).

where the Einstein summation convention for like indices is assumed, and we have dropped terms $\mathcal{O}(1/\Lambda^2)$. In this equation there are terms that have \sqrt{mE} dependence, which we distinguish from $|\mathbf{p}|$ because we keep the atoms off the mass shell in our calculations, *i.e.* $E \neq \frac{\mathbf{p}^2}{m}$. Each term in Eq. (36) will be matched to the matrix elements of the relevant local operators, and by this matching process the Wilson coefficients of the local operators will be determined. $\mathcal{A}^2(E)$ is the renormalized square amplitude and includes the correction due to the finite effective range. But, Eq. (36) is still valid in the zero range limit, in which we replace $\mathcal{A}(E)$ by \mathcal{A}_{LO} . With the r^3 term still present, this confirms that the $1/k^6$ correction to the tail of the momentum distribution is still present even when $r_s \rightarrow 0$.

Next, we calculate the matrix elements of local operators for the two-body scattering state. As in the calculation for the nonlocal operator, we do not drop power-suppressed terms in the amplitude Eq. (33) during intermediate steps, and we keep terms up to NLO in the EFT expansion after the renormalization.

A. One-body local operators

In this subsection, we calculate matrix elements for the one-body operators of various scaling dimensions $\mathcal{O}_{1,\Delta}$ in Eq. (30). The Feynman diagrams in Fig. 6 show all contributions for the two-atom scattering state. The first diagram contributes even in the absence of two-body interactions.

Since Fig. 6 is the same for any one-body operator, its matrix element can be written as:

$$\langle \mathcal{O}_{1,\Delta} \rangle = v_{1,\Delta}(\mathbf{p}) \delta_{\mathbf{p}\mathbf{k}} - \left[\frac{v_{1,\Delta}(\mathbf{p}) \mathcal{A}(E)}{p_0 - \mathbf{p}^2/(2m)} + (p \rightarrow k) \right] - \mathcal{I}_0^{(1,\Delta)} \mathcal{A}^2(E) - 2 \left[\left(\frac{\mathbf{p}^2 + \mathbf{k}^2}{2} - 2mE \right) \mathcal{I}_0^{(1,\Delta)} + \mathcal{I}_2^{(1,\Delta)} \right] \mathcal{A}_\lambda \mathcal{A}_{\rho'}. \quad (37)$$

where $v_{1,\Delta}(\mathbf{p})$ is the vertex factor for the operator $\mathcal{O}_{1,\Delta}$. The vertex factors up to dimension 6 are given in Table III in the Appendix. The loop integrals $\mathcal{I}_{2n}^{(1,\Delta)}$ are also found in the Appendix in Eq. (A4).

The matrix element of $\mathcal{O}_{1,3} = \psi_\sigma^\dagger \psi_\sigma$ for a two-body state and ingoing momentum \mathbf{p} and outgoing momentum

\mathbf{k} is

$$\langle \mathcal{O}_{1,3} \rangle = \delta_{\mathbf{p}\mathbf{k}} - \left[\frac{\mathcal{A}(E)}{p_0 - \mathbf{p}^2/(2m)} + (p \rightarrow k) \right] + \frac{im^2 \mathcal{A}^2(E)}{8\pi\sqrt{mE}} \left(1 + ir_s \sqrt{mE} \right) + \mathcal{O}(\Lambda^{-2}). \quad (38)$$

Note that $r_s \mathcal{A}^2(E) = r_s \mathcal{A}_\lambda^2$ up to NLO in r_s .

Except for the term proportional to r_s , Eq. (38) is matched to the second line of Eq. (36), and the Wilson coefficient is

$$W_{1,3} = 1. \quad (39)$$

The r_s term will be subtracted later by including an appropriate term in the Wilson coefficient of the 2-body operator in Eq. (49).

Next, the matrix element of $\mathcal{O}_{1,4} = \psi_\sigma^\dagger \overleftrightarrow{\partial}_i \psi_\sigma$ is given by

$$\langle \mathcal{O}_{1,4} \rangle = 2ip_i \delta_{\mathbf{p}\mathbf{k}} - \left[\frac{2ip_i \mathcal{A}(E)}{p_0 - \mathbf{p}^2/(2m)} + (p \rightarrow k) \right]. \quad (40)$$

By comparing this to terms containing one power of p_i in Eq. (36), it is clear that the Wilson coefficient corresponding to $\mathcal{O}_{1,4}$ is given by

$$W_{1,4} = \frac{1}{2} r_i. \quad (41)$$

The next operator is $\mathcal{O}_{1,5} = \psi_\sigma^\dagger \overleftrightarrow{\partial}_i \overleftrightarrow{\partial}_j \psi_\sigma$ and its matrix element is given by

$$\langle \mathcal{O}_{1,5} \rangle = -4p_i p_j \delta_{\mathbf{p}\mathbf{k}} + \left[\frac{4p_i p_j \mathcal{A}(E)}{p_0 - \mathbf{p}^2/(2m)} + (p \rightarrow k) \right] - \frac{4\delta_{ij}}{3} \left[i \frac{d\mathcal{I}_2}{dE} \right] \mathcal{A}^2(E) - \frac{4m\delta_{ij}}{3} \left[\frac{m\Lambda^3}{3\pi^2} + \left(\frac{\mathbf{p}^2 + \mathbf{k}^2}{m} - 2E \right) i \frac{d\mathcal{I}_2}{dE} + 2imE\mathcal{I}_0 \right] \mathcal{A}_\lambda \mathcal{A}_{\rho'}. \quad (42)$$

Note that this matrix element is linearly divergent, with $\Lambda^3 \mathcal{A}_{\rho'} \sim \Lambda$, and we will renormalize this divergence and other explicit Λ -dependence by adding the two-body operators $\psi_1^\dagger \psi_2^\dagger \psi_2 \psi_1$ and $\psi_1^\dagger \psi_2^\dagger \psi_2 \overleftrightarrow{\nabla}^2 \psi_1$ with appropriate factors. The operator $\psi_\sigma^\dagger \overleftrightarrow{\partial}_i \overleftrightarrow{\partial}_j \psi_\sigma$ with i, j contracted becomes the kinetic term in the Hamiltonian and the cutoff dependence implies that the kinetic energy is sensitive to the short-distance region of a fundamental potential smaller than the length scale $a \sim 1/\sqrt{mE}$ beyond which our effective theory loses predictive power. Through this renormalization procedure, we find combinations of operators that are insensitive to the short-distance behavior.

Δ	$\mathcal{O}_{1,\Delta}$	$W_{1,\Delta}$
3	$\psi_\sigma^\dagger \psi_\sigma$	1
4	$\psi_\sigma^\dagger \overleftrightarrow{\partial}_i \psi_\sigma$	$\frac{1}{2} r_i$
5	$\psi_\sigma^\dagger \overleftrightarrow{\partial}_i \overleftrightarrow{\partial}_j \psi_\sigma^{(\text{ren})}$	$\frac{1}{8} r_i r_j$
6	$\psi_\sigma^\dagger \overleftrightarrow{\partial}_i \overleftrightarrow{\partial}_j \overleftrightarrow{\partial}_k \psi_\sigma$	$\frac{1}{48} r_i r_j r_k$

TABLE I: One-body operators up to scaling dimension 6 and their Wilson coefficients $W_{1,\Delta}$, where the 1 corresponds to one-body and the Δ corresponds to the dimensionality of the operator.

By using the renormalized two-body operators found in Subsection 2 below in Eqs. (49) and (54), we obtain the result for the renormalized operator $\mathcal{O}_{1,5}$

$$\begin{aligned}
\langle \mathcal{O}_{1,5}^{(\text{ren})} \rangle &= \left\langle \mathcal{O}_{1,5} + \frac{2\delta_{ij}}{3\pi^2} \left[\Lambda \left(1 + \frac{2z}{3} \right) \mathcal{O}_{2,4}^{(\text{ren})} + \frac{1-3z}{4\Lambda} \mathcal{O}_{2,6}^{(\text{ren})} \right] \right\rangle \\
&= -4p_i p_j \delta_{\mathbf{p}\mathbf{k}} + \left[\frac{4p_i p_j \mathcal{A}(E)}{p_0 - \mathbf{p}^2/(2m)} + (p \rightarrow k) \right] \\
&\quad - i\delta_{ij} \frac{\sqrt{mE}}{2\pi} m^2 \mathcal{A}^2(E) + O(\Lambda^{-2}). \tag{43}
\end{aligned}$$

Here $z = \frac{m\rho_0\Lambda^2}{\lambda_0}$ and the superscript (ren) indicates a renormalized operator, which has its UV divergence content properly regularized and renormalized. By comparing Eq. (43) to the $O(r^2)$ terms in Eq. (36), we find this operator's Wilson coefficient to be

$$W_{1,5} = \frac{1}{8} r_i r_j. \tag{44}$$

Lastly, the matrix element of $\mathcal{O}_{1,6} = \psi_\sigma^\dagger \overleftrightarrow{\partial}_i \overleftrightarrow{\partial}_j \overleftrightarrow{\partial}_k \psi_\sigma$ is given by

$$\langle \mathcal{O}_{1,6} \rangle = -i8p_i p_j p_k \delta_{\mathbf{p}\mathbf{k}} + \left[\frac{i8p_i p_j p_k \mathcal{A}(E)}{p_0 - \mathbf{p}^2/(2m)} + (p \rightarrow k) \right]. \tag{45}$$

No renormalization is necessary for this operator. Comparing this to the terms of $O(r^3)$ in Eq. (36), we get its Wilson coefficient:

$$W_{1,6} = \frac{1}{48} r_i r_j r_k. \tag{46}$$

B. Two-Body Local Operators

In this subsection we calculate the matrix elements of the two-body operators $\mathcal{O}_{2,\Delta}$ for two-atom scattering states and determine their Wilson coefficients, $W_{2,\Delta}$. Figure 7 shows the relevant diagrams for the two-body scattering state. The operators of dimensions $\Delta = 4, 6$

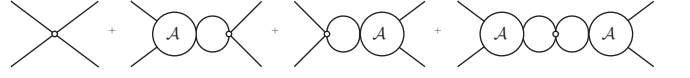


FIG. 7: Diagrams for 2-body operators (empty dot).

are those which are relevant for the momentum distribution and other universal relations.

Since Fig. 7 is the same for any 2-body operators, its matrix element can be written generally as

$$\begin{aligned}
\langle \mathcal{O}_{2,\Delta} \rangle &= (1 + i\mathcal{I}_0 \mathcal{A}(E)) [v_{2,\Delta}(p, k) + 2i\mathcal{I}_0^{(2,\Delta)} \mathcal{A}(E)] \\
&\quad + i\mathcal{A}_{\rho'} \left\{ 2\mathcal{I}_2^{(2,\Delta)} (1 + i\mathcal{I}_0 \mathcal{A}_\lambda) \right. \\
&\quad + \mathcal{I}_2 [v_{2,\Delta}(p, k) + 2i\mathcal{I}_0^{(2,\Delta)} \mathcal{A}_\lambda] \\
&\quad + (\mathbf{p}^2 + \mathbf{k}^2 - 4mE)(1 + 2i\mathcal{I}_0 \mathcal{A}_\lambda) \mathcal{I}_0^{(2,\Delta)} \\
&\quad \left. + [v_{2,\Delta}(p)(\mathbf{k}^2 - 2mE) + v_{2,\Delta}(k)(\mathbf{p}^2 - 2mE)] \mathcal{I}_0 \right\}, \tag{47}
\end{aligned}$$

where $v_{2,\Delta}(p, k) = v_{2,\Delta}(p) + v_{2,\Delta}(k)$ is the vertex factor for the operator $\mathcal{O}_{2,\Delta}$, and up to scaling dimension 6 these factors are given in Table IV in the Appendix. For convenience, the vertex factors are broken up into terms depending on a vertex's ingoing and outgoing momenta. Thus, the factors can depend either on the external momentum or the loop momentum of the particles. Loop momentum-dependent terms are included in the integrals defined by Eq. (A7) in the Appendix. The integrals \mathcal{I}_0 and \mathcal{I}_2 are defined in the Appendix by Eq. (A1). One important note is that $\mathcal{O}_{2,4}$ has the momentum-independent vertex factor $v_{2,4}(p, k) = 1$. This is broken up into $v_{2,4}(p) = 1/2$ and $v_{2,4}(k) = 1/2$ simply to follow the prescription given by Eq. (47). Also, one is not allowed to directly use the LS equation to simplify $(1 + i\mathcal{I}_0 \mathcal{A})$ in the above equation because $\mathcal{A}(E) = \mathcal{A}_\lambda + \mathcal{A}_\rho$ here. The LS equation only includes \mathcal{A}_λ . Additionally, any factors of $\mathcal{A}(E)$ multiplying $\mathcal{A}_{\rho'}$ are \mathcal{A}_λ , rather than $\mathcal{A}_\lambda + \mathcal{A}_\rho$, since we only want terms up to NLO in ρ_0 , or r_s .

The leading two-body operator $\mathcal{O}_{2,4} = \psi_1^\dagger \psi_2^\dagger \psi_2 \psi_1$ has been already calculated in the zero-range model [8] and the field theoretical two-channel model for a narrow Feshbach resonance [21]. Its matrix element is given by

$$\begin{aligned}
\langle \mathcal{O}_{2,4} \rangle &= (1 + i\mathcal{I}_0 \mathcal{A}(E))^2 \\
&\quad + i\mathcal{A}_{\rho'} (1 + i\mathcal{I}_0 \mathcal{A}_\lambda) [2\mathcal{I}_2 + (\mathbf{p}^2 + \mathbf{k}^2 - 4mE) \mathcal{I}_0]. \tag{48}
\end{aligned}$$

With a multiplicative factor λ_0^2 we obtain a renormalized operator $\lambda_0^2 \psi_1^\dagger \psi_2^\dagger \psi_2 \psi_1$ at LO in [8, 21]. Similarly at NLO, it is renormalized by a multiplicative factor as

$$\begin{aligned}
\langle \mathcal{O}_{2,4}^{(\text{ren})} \rangle &= \left\langle \lambda_0^2 \left(1 + \frac{m\rho_0\Lambda^3}{3\pi^2} \right) \mathcal{O}_{2,4} \right\rangle \\
&= m^2 \mathcal{A}^2(E) + 2m\lambda_0 \mathcal{A}_\rho - i(\mathbf{p}^2 + \mathbf{k}^2 - 2mE) m^2 \rho_0 \mathcal{I}_0 \mathcal{A}_\lambda^2 \\
&= m^2 \mathcal{A}^2(E) + O(\Lambda^{-2}), \tag{49}
\end{aligned}$$

where we used the LS equation in Eq. (34) to eliminate $1 + \mathcal{I}_0 i\mathcal{A}_\lambda$ in favor of $-m\mathcal{A}_\lambda/\lambda_0$. As shown in the last expression, we drop terms $\sim 1/\Lambda^2$. Note that the operator $\mathcal{O}_{2,4}^{(\text{ren})}$ is \mathcal{O}_C , the contact density operator.

This can be compared to the third term proportional to r in Eq. (36), and this operator's Wilson coefficient is given by

$$W_{2,4} = -\frac{r}{8\pi} + \frac{r_s}{8\pi}, \quad (50)$$

where we need the term proportional to r_s here to cancel the term proportional to r_s in the one-body result in Eq. (38), as discussed before. Note that for $\mathcal{O}_{1,3}$ we did not write $\mathcal{O}_{1,3}^{(\text{ren})} = \mathcal{O}_{1,3} + \frac{r_s}{8\pi}\lambda_0^2\mathcal{O}_{2,4}$. This is because the matrix element $\langle \mathcal{O}_{1,3} \rangle$ is finite with no explicit Λ -dependence, so renormalization is not the proper procedure to eliminate the extra term. On the other hand, the extra term needs to be canceled, so we use the Wilson coefficient of $\mathcal{O}_{2,4}$ to accomplish this by adding the term proportional to r_s in Eq. (50).

The matrix element of $\mathcal{O}_{2,5} = \psi_1^\dagger \psi_2^\dagger \psi_2 \overleftrightarrow{\partial}_i \psi_1 + h.c.$ is simple because $\mathcal{I}_{2n}^{(2,5)} = 0$.

$$\begin{aligned} \langle \mathcal{O}_{2,5} \rangle &= 2i(p_i + k_i)[1 + i\mathcal{I}_0 \mathcal{A}(E)] \\ &- 2\mathcal{A}_{\rho'} \left\{ (p_i + k_i)\mathcal{I}_2 + [p_i(\mathbf{k}^2 - 2mE) + k_i(\mathbf{p}^2 - 2mE)]\mathcal{I}_0 \right\}. \end{aligned} \quad (51)$$

This operator is renormalized by a multiplicative factor as

$$\begin{aligned} \langle \mathcal{O}_{2,5}^{(\text{ren})} \rangle &= \langle \lambda_0 \left(1 + \frac{m\rho_0\Lambda^3}{6\pi^2} \right) \mathcal{O}_{2,5} \rangle, \\ &= -2i(p_i + k_i)m\mathcal{A}(E) + O(\Lambda^{-2}). \end{aligned} \quad (52)$$

But, this matrix element is not matched to any term in Eq. (36) and its Wilson coefficient is thus $W_{2,5} = 0$.

For the operator $\psi_1^\dagger \psi_2^\dagger \psi_2 \overleftrightarrow{\partial}_i \overleftrightarrow{\partial}_j \psi_1 + h.c.$, we define $\mathcal{O}_{2,6}$ as this operator contracted with δ_{ij} because then it matches to the terms in the matrix element of the nonlocal operator in Eq. (36).

$$\begin{aligned} \langle \mathcal{O}_{2,6} \rangle &= -4(1 + i\mathcal{I}_0 \mathcal{A}(E))(\mathbf{p}^2 + \mathbf{k}^2 + 2i\mathcal{I}_2 \mathcal{A}(E)) \\ &- 4i\mathcal{A}_{\rho'} \left\{ 2(1 + i\mathcal{I}_0 \mathcal{A}_\lambda)\mathcal{I}_4 + (\mathbf{p}^2 + \mathbf{k}^2 + 2i\mathcal{I}_2 \mathcal{A}_\lambda)\mathcal{I}_2 \right. \\ &\quad + (\mathbf{p}^2 + \mathbf{k}^2 - 4mE)(1 + 2i\mathcal{I}_0 \mathcal{A}_\lambda)\mathcal{I}_2 \\ &\quad \left. + [\mathbf{p}^2(\mathbf{k}^2 - 2mE) + \mathbf{k}^2(\mathbf{p}^2 - 2mE)]\mathcal{I}_0 \right\}. \end{aligned} \quad (53)$$

To renormalize $\mathcal{O}_{2,6}$, we use momentum-dependent operators only, and work in the on-shell limit, where $\mathbf{p}^2 = \mathbf{k}^2 = mE$, which allows us to avoid energy de-

Δ	$\mathcal{O}_{2,\Delta}$	$W_{2,\Delta}$
4	$\psi_1^\dagger \psi_2^\dagger \psi_2 \psi_1^{(\text{ren})}$	$-\frac{r-r_s}{8\pi}$
5	$\psi_1^\dagger \psi_2^\dagger \psi_2 \overleftrightarrow{\partial}_i \psi_1^{(\text{ren})} + h.c.$	0
6	$\psi_1^\dagger \psi_2^\dagger \psi_2 \overleftrightarrow{\nabla}^2 \psi_1^{(\text{ren})} + h.c.$	$-\frac{r^3}{384\pi}$

TABLE II: Two-body operators $\mathcal{O}_{2,\Delta}$ up to scaling dimension 6 and their Wilson coefficients.

pendent operators.

$$\begin{aligned} \langle \mathcal{O}_{2,6}^{(\text{ren})} \rangle &= \left\langle \lambda_0^2 \left(1 + \frac{3}{2}x \right) \mathcal{O}_{2,6} \right. \\ &\quad \left. - \left[\frac{4\lambda_0^3\Lambda^3}{3\pi^2} (1 + 2x) + \frac{12\lambda_0^2\Lambda^2x}{5} \right] \mathcal{O}_{2,4} \right\rangle \quad (54) \\ &= -8mEm^2\mathcal{A}^2(E) + O(\Lambda^{-2}), \end{aligned} \quad (55)$$

where $x = \frac{\rho_0 m \Lambda^3}{3\pi^2}$. The operators for the contact C and derivative contact D in Eq. (13) are related to the renormalized operators as

$$\mathcal{O}_{2,4}^{(\text{ren})} = \mathcal{O}_C, \quad (56)$$

$$\mathcal{O}_{2,6}^{(\text{ren})} = -4\mathcal{O}_D. \quad (57)$$

This equality is seen when we drop the factors of ρ_0 in Eq. (54) and compare to Eq. (65), as there is already a factor of ρ_0 in the Hamiltonian and we are only treating the problem to NLO in r_s . Then, Eq. (54) is matched to the last r^3 term in Eq. (36) with the following Wilson coefficient:

$$W_{2,6} = -\frac{r^3}{384\pi}. \quad (58)$$

The Wilson coefficients for the two-body operators are compiled in Table II.

Now we generalize our results by considering a two-body system with a finite center-of-mass momentum \mathbf{K} . The relative momentum of each particle remains $\pm\mathbf{p}$. The single particle momentum, expressed in terms of center-of-mass and relative momenta, is $\mathbf{K}/2 \pm \mathbf{p}$. In addition to this momentum shift by $\mathbf{K}/2$, the total energy E is replaced by the Galilean invariant energy $E - \mathbf{K}^2/4m$. The boost results in the multiplicative factor $e^{i\mathbf{K}\cdot\mathbf{r}/2}$ in Eq. (35) and can be reproduced in the OPE by appropriate operators. The one-body results in Table I can be written in the compressed form $\psi_\sigma^\dagger e^{\mathbf{r}\cdot\overleftrightarrow{\partial}/2} \psi_\sigma$ to reproduce this factor. In the two-body sector, we can account for a finite center-of-mass momentum in the OPE by including the operator $\psi_1^\dagger \psi_2^\dagger \psi_2 e^{\mathbf{r}\cdot\overleftrightarrow{\partial}/2} \psi_1$ in place of $\mathcal{O}_{2,4}$, where $\overleftrightarrow{\partial}_i = \overrightarrow{\partial}_i + \overleftarrow{\partial}_i$. We can expand the exponential in small r and define two new operators up to scaling dimension 6:

$$\begin{aligned} \mathcal{O}'_{2,5} &= 2i \psi_1^\dagger \psi_2^\dagger \psi_2 \overleftrightarrow{\partial}_i \psi_1^{(\text{ren})}, \\ \mathcal{O}'_{2,6} &= -\frac{1}{2} \psi_1^\dagger \psi_2^\dagger \psi_2 \overleftrightarrow{\partial}_i \overleftrightarrow{\partial}_j \psi_1^{(\text{ren})}. \end{aligned}$$

Note that the Wilson coefficients are trivial in the sense that, after including the appropriate factors from the definitions of $\mathcal{O}'_{2,5}$ and $\mathcal{O}'_{2,6}$, we simply use the coefficient $W_{2,4}$.

C. The Momentum Distribution and the Hamiltonian

Collecting all the one- and two-body matching results and Fourier transforming to momentum space, we obtain

$$\begin{aligned} \rho_\sigma(\mathbf{k}) &= \int_{\mathbf{R}} \int_{\mathbf{r}} e^{i\mathbf{k}\cdot\mathbf{r}} \langle \psi_\sigma^\dagger(\mathbf{R} - \mathbf{r}/2) \psi_\sigma(\mathbf{R} + \mathbf{r}/2) \rangle \\ &= \int_{\mathbf{R}} \left\{ \delta_{\mathbf{k}} \langle \mathcal{O}_{1,3}(\mathbf{R}) \rangle - i \frac{\nabla_{k_i} \delta_{\mathbf{k}}}{2} \langle \mathcal{O}_{1,4}(\mathbf{R}) \rangle - \frac{\nabla_{k_i} \nabla_{k_j} \delta_{\mathbf{k}}}{8} \langle \mathcal{O}_{1,5}^{(\text{ren})}(\mathbf{R}) \rangle + i \frac{\nabla_{k_i} \nabla_{k_j} \nabla_{k_k} \delta_{\mathbf{k}}}{48} \langle \mathcal{O}_{1,6}(\mathbf{R}) \rangle \right. \\ &\quad + \left(\frac{1}{k^4} + r_s \frac{\delta_{\mathbf{k}}}{8\pi} \right) \langle \mathcal{O}_C(\mathbf{R}) \rangle + \frac{1}{k^6} \langle \mathcal{O}_D(\mathbf{R}) \rangle \\ &\quad \left. + \left(\frac{\hat{k}_i}{k^5} - r_s \frac{\nabla_{k_i} \delta_{\mathbf{k}}}{32\pi} \right) \langle \mathcal{O}'_{2,5}(\mathbf{R}) \rangle + \left(\frac{6\hat{k}_i \hat{k}_j - \delta_{ij}}{k^6} + r_s \frac{\nabla_{k_i} \nabla_{k_j} \delta_{\mathbf{k}}}{32\pi} \right) \langle \mathcal{O}'_{2,6}(\mathbf{R}) \rangle \right\}, \end{aligned} \quad (59)$$

where $\int_{\mathbf{R}} = \int d^3\mathbf{R}$, $\int_{\mathbf{r}} = \int d^3\mathbf{r}$, $\delta_{\mathbf{k}} = (2\pi)^3 \delta^{(3)}(\mathbf{k})$, and the unit vector $\hat{k}_i = k_i/k$. The third line in Eq. (59) corresponds to the contact C and derivative contact D in Eq. (13). On the last line the term with the $1/k^6$ tail corresponds to the term $C' \equiv \int_{\mathbf{R}} \delta_{ij} \langle \mathcal{O}'_{2,6}(\mathbf{R}) \rangle$ in Eq. (13) after an angular average over \mathbf{k} , while the term with $1/k^5$ tail vanishes.

For the derivation of the energy relation in Eq. (14) we first write the Hamiltonian in the absence of an external potential, using the terms from the Lagrangian in Eqs. (4) and (5) as $H = H_0 + H_1$, where

$$\begin{aligned} H_0 &= \int_{\mathbf{R}} \left[\mathcal{T}(\mathbf{R}) + \frac{\lambda_0}{m} \mathcal{O}_{2,4}(\mathbf{R}) \right], \\ H_1 &= \int_{\mathbf{R}} \left[\frac{-\rho_0}{4} \mathcal{O}_{2,6}(\mathbf{R}) + \frac{\delta\lambda_0}{m} \mathcal{O}_{2,4}(\mathbf{R}) \right]. \end{aligned} \quad (60)$$

Then we rewrite the operators in the Hamiltonian in terms of the operators that appear in Eq. (13):

$$H_0 = \int_{\mathbf{R}} \left[\mathcal{T} + \frac{\mathcal{O}_C}{4\pi m a} - \left(\frac{\Lambda}{2\pi^2 m} + \frac{\rho_0 \Lambda^3}{3\pi^2 \lambda_0} \right) \mathcal{O}_C \right], \quad (61)$$

$$H_1 = \int_{\mathbf{R}} \frac{\rho_0}{\lambda_0^2} \mathcal{O}_D = \int_{\mathbf{R}} \frac{1}{16\pi m} \left(r_s - \frac{4}{\pi \Lambda} \right) \mathcal{O}_D. \quad (62)$$

The operators \mathcal{T} , \mathcal{O}_C , and \mathcal{O}_D are

$$\mathcal{T}(\mathbf{R}) \equiv \frac{1}{2m} \sum_{\sigma} \nabla \psi_{\sigma}^{\dagger} \cdot \nabla \psi_{\sigma}, \quad (63)$$

$$\mathcal{O}_C(\mathbf{R}) \equiv \mathcal{O}_{2,4}^{(\text{ren})} = \lambda_0^2 \left(1 + \frac{m\rho_0\Lambda^3}{3\pi^2} \right) \mathcal{O}_{2,4}, \quad (64)$$

$$\mathcal{O}_D(\mathbf{R}) \equiv -\frac{\mathcal{O}_{2,6}^{(\text{ren})}}{4} = -\frac{\lambda_0^2}{4} \left[\mathcal{O}_{2,6} - \frac{4\lambda_0\Lambda^3}{3\pi^2} \mathcal{O}_{2,4} \right] + O(\rho_0), \quad (65)$$

where λ_0 and ρ_0 are the bare couplings related to the scattering length a and effective range r_s as shown in Eqs. (8) and (11). Note that in Eq. (65) we were able to drop all terms proportional to ρ_0 that appear in the definition of $\mathcal{O}_{2,6}^{(\text{ren})}$ because there is already a factor of ρ_0 multiplying \mathcal{O}_D in the finite range part of the Hamiltonian given by Eq. (62), and terms proportional to ρ_0^2 should be dropped since we are working only up to NLO in the range. We use Eq. (11) to rewrite H_1 into a term proportional to $r_s \mathcal{O}_D$ and a term proportional to $\frac{1}{\Lambda} \mathcal{O}_D$.

The last term in square brackets in Eq. (65) is a counter term which subtracts the divergent part of the matrix element (\mathcal{O}_D). This performs the same task as the term proportional to $\delta\lambda_0$ in the Lagrangian described in Sec. II. Furthermore, we see that in this case $\frac{\rho_0}{\lambda_0^2} \mathcal{O}_D$ and $\frac{-\rho_0}{4\lambda_0^2} \mathcal{O}_{2,6}^{(\text{ren})}$, using Eq. (54), give the same result in the Hamiltonian.

The subtracted kinetic term $T^{(\text{sub})}$ in Eq. (14) is defined by absorbing the explicit cutoff dependence from

H_0 and H_1 into the kinetic term as

$$\langle T^{(\text{sub})} \rangle = \int_{\mathbf{R}} \left\langle \mathcal{T} - \frac{1}{2\pi^2 m} \left[\Lambda \left(1 + \frac{2m\rho_0\Lambda^2}{3\lambda_0} \right) \mathcal{O}_C + \frac{\mathcal{O}_D}{2\Lambda} \right] \right\rangle. \quad (66)$$

$T^{(\text{sub})}$ contains the terms proportional to $\Lambda\mathcal{O}_C, \Lambda^3\mathcal{O}_C$ to subtract the divergent pieces of $\int_{\mathbf{R}} \langle \mathcal{T} \rangle$ and the term proportional to $\frac{1}{\Lambda}\mathcal{O}_D$, as mentioned above, to remove the remaining Λ -dependence.

VI. CONCLUSION

In this paper we carried out the operator product expansion for the momentum distribution of a two-component Fermi gas including all terms that are first order in the effective range. Using the result for the momentum distribution of a two-particle scattering state, we matched all operators up to scaling dimension 6 and obtained the corresponding Wilson coefficients. We used a sharp cutoff in our calculations and used an EFT framework to include corrections due to a finite effective range.

The main results of this work are extended universal relations that contain the previously known contact C and the two quantities C' and D . Specifically, their sum appears as the asymptote of the subleading $(C' + D)/k^6$ tail in the momentum distribution. The derivative contact D alone also appears in universal relations for the total energy, its derivative with respect to the effective range r_s , the pressure relation, and the virial theorem as an effective range correction of the form $r_s D$. Werner and Castin [22] first found the subleading tail and its relation to energy $D = 16\pi m dE/dr_s$, which we reproduced using the OPE.

While effective range corrections to observables are generally suppressed by a factor of r_s/a , the size of derivative contact itself is not suppressed in this way in comparison to the size of contact. For instance, the QMC simulation in Ref. [28] obtained, in the unitary limit, the density of the derivative contact $\mathcal{D}/k_F^6 \approx 0.06$, while the contact density is $\mathcal{C}/k_F^4 \approx 0.11$. In the BEC limit ($a \rightarrow 0^+$), the derivative contact becomes more important because it scales like $\mathcal{D}/k_F^6 \propto 1/(k_F a)^3$, while the contact scales like $\mathcal{C}/k_F^4 \propto 1/(k_F a)$. Our result for the tail of the momentum distribution, in the absence of a known value for C' , already improves the description of the numerical many-body calculation for the same quantity for $k > 1.5k_F$ as shown in Fig. 4. The subleading \mathcal{D}/k^6 in the tail gives a correction as large as 20% near $1.5k_F$ in unitary limit.

Our results are the first step towards range-corrected universal relations for other observables such as the single-particle dispersion relation, structure factors, and RF spectroscopy. In our calculation we have not considered the 3-body operator that would lead to the Efimov effect and a $1/k^5$ tail for the large imbalanced mass ratio $m_1/m_2 > 13.6$ [47] or in a system of three identical

bosons [14]. This would be an interesting extension of the work presented here.

Acknowledgements

We thank J. Carlson and S. Gandolfi for providing their QMC results and E. Mereghetti for helpful discussions. We thank E. Braaten for comments and Y. Castin, and F. Werner for their feedback on the manuscript. DK would like to thank the University of Tennessee, Knoxville for hospitality while this work was started. This work was supported by the U.S. Department of Energy through the Office of Science, Office of Nuclear Physics under Contract Nos. DE-AC52-06NA25396, DE-AC05-00OR22725, an Early Career Research Award, the LANL/LDRD Program, and by the National Science Foundation under Grant No. PHY-1516077.

Δ	3	4	5	6
$v_{1,\Delta}(\mathbf{p})$	1	$2ip_i$	$-4p_i p_j$	$-8ip_i p_j p_k$

TABLE III: Vertex Factors for 1-body operators of $\Delta = 3..6$.

Appendix A: Vertex Factors and Loop Integrals

In the calculation of the scattering amplitude we encounter the loop diagrams shown in Fig. 2 which lead to the integrals $\mathcal{I}_{2n}(E)$:

$$\begin{aligned} \mathcal{I}_{2n}(E, \Lambda) &= \int_q \frac{i\mathbf{q}^{2n}}{q_0 - \frac{\mathbf{q}^2}{2m} + i\epsilon} \frac{i}{E - q_0 - \frac{\mathbf{q}^2}{2m} + i\epsilon} \\ &= -\frac{im\Lambda^{2n+1}}{2(2n+1)\pi^2} + mE \mathcal{I}_{2n-2}(E, \Lambda), \quad (\text{A1}) \end{aligned}$$

$$\begin{aligned} \mathcal{I}_0(E, \Lambda) &= -\frac{im}{2\pi^2} \left(\Lambda + \frac{\sqrt{mE}}{2} \left[i\pi + \ln \left(\frac{\Lambda - \sqrt{mE}}{\Lambda + \sqrt{mE}} \right) \right] \right) \\ &\approx -\frac{im}{2\pi^2} \left(\Lambda + \frac{i\pi}{2} \sqrt{mE} - \frac{mE}{\Lambda} + \dots \right), \quad (\text{A2}) \end{aligned}$$

$$\begin{aligned} \mathcal{I}_2(E, \Lambda) &\approx -\frac{im}{2\pi^2} \left(\frac{\Lambda^3}{3} + mE\Lambda + \frac{i\pi}{2} (mE)^{3/2} \right. \\ &\quad \left. - \frac{(mE)^2}{\Lambda} + \dots \right), \quad (\text{A3}) \end{aligned}$$

where the integral symbol is defined as $\int_q = \int \frac{d^4q}{(2\pi)^4}$. We assume $E > 0$ because we carry out the matching for the two-atom scattering state above the threshold. The result which is valid above and below the threshold is given in [48]. The even powers of \mathbf{q} in the numerator of $\mathcal{I}_{2n}(E, \Lambda)$, indicated by the index $2n$, come from the attachment of the part of the off shell amplitude with explicit momentum dependence to a loop diagram.

Next, we examine the integrals which arise in the one-body operator loop diagrams. Depending upon the particular operator under consideration, the vertex factor in the loop integrals changes, and Table III below shows the one-body vertex factors. These factors, as well as the various $v_{2,\Delta}(q, l)$, can be derived by inserting the definition of the nonrelativistic fermion field into the operators listed in Eq. (30) and taking the given spatial derivatives.

The loop integral $\mathcal{I}_{2n}^{(1,\Delta)}$, for which Table III applies, is from the last Feynman diagram of Fig. 6 and is given by

$$\begin{aligned} \mathcal{I}_{2n}^{(1,\Delta)}(E) &= \int_q \frac{i^2 \mathbf{q}^{2n} v_{1,\Delta}(\mathbf{q})}{[E - q_0 - \frac{\mathbf{q}^2}{2m} + i\epsilon]^2} \frac{i}{q_0 - \frac{\mathbf{q}^2}{2m} + i\epsilon} \\ &= -i \frac{d}{dE} \left[\int_q \frac{i\mathbf{q}^{2n} v_{1,\Delta}(\mathbf{q})}{E - q_0 - \frac{\mathbf{q}^2}{2m} + i\epsilon} \frac{i}{q_0 - \frac{\mathbf{q}^2}{2m} + i\epsilon} \right]. \quad (\text{A4}) \end{aligned}$$

The subscript $2n$ in $\mathcal{I}_{2n}^{(1,\Delta)}(E)$ indicates the number of powers of \mathbf{q} in the numerator of the integral due to the attachment of the off shell amplitude, and the superscript $(1, \Delta)$ specifies that this integral corresponds to the insertion of a one-body operator of dimension Δ into a loop

Δ	4	5	6
$v_{2,\Delta}(\mathbf{p})$	$1/2$	$2ip_i$	$-4\delta_{ij} p_i p_j$

TABLE IV: Partial vertex factors for two-body operators of dimensions $\Delta = 4..6$. For the total vertex factor, one must use $v_{2,\Delta}(q, l) = v_{2,\Delta}(q) + v_{2,\Delta}(l)$, where q and l are the vertex's ingoing and outgoing momentum, respectively. The δ_{ij} comes from the use of ∇^2 rather than $\partial_i \partial_j$ in $\mathcal{O}_{2,6}$.

diagram. Inserting the factors $v_{1,\Delta}(\mathbf{q})$ given in Table III into Eq. (A4) gives

$$\mathcal{I}_{2n}^{(1,3)}(E) = -i \frac{d\mathcal{I}_{2n}(E)}{dE}, \quad (\text{A5})$$

$$\mathcal{I}_{2n}^{(1,5)}(E) = i \frac{4\delta_{ij}}{3} \frac{d\mathcal{I}_{2n+2}(E)}{dE}, \quad (\text{A6})$$

where $\mathcal{I}_{2n}^{(1,\Delta)}(E) = 0$ for even $\Delta = 4, 6$ because their integrand is an odd function of \mathbf{q} . By using \mathcal{I}_{2n} given in Eq. (A1), we obtain explicit expressions for $\mathcal{I}_{2n}^{(1,\Delta)}$.

For two-body operators, the integrals $\mathcal{I}_{2n}^{(2,\Delta)}$ represent loop integrals useful in the diagrammatic calculations of Fig. 7.

$$\mathcal{I}_{2n}^{(2,\Delta)}(E) = \int_q \frac{i\mathbf{q}^{2n} v_{2,\Delta}(\mathbf{q})}{q_0 - \frac{\mathbf{q}^2}{2m} + i\epsilon} \frac{i}{E - q_0 - \frac{\mathbf{q}^2}{2m} + i\epsilon}. \quad (\text{A7})$$

Inserting the vertex factors $v_{2,\Delta}$ from Table IV into Eq. (A7) gives

$$\mathcal{I}_{2n}^{(2,4)}(E) = \frac{\mathcal{I}_{2n}(E)}{2}, \quad (\text{A8})$$

$$\mathcal{I}_{2n}^{(2,6)}(E) = -\frac{4\delta_{ij}}{3} \mathcal{I}_{2n+2}(E), \quad (\text{A9})$$

while $\mathcal{I}_{2n}^{(2,5)}(E) = 0$. The even powers of loop momentum in the integrals again come from the attachment of the momentum-dependent part of the off shell amplitude to loop diagrams. Additional powers of momentum may be added to the numerator in Eq. (A7) by the vertex factors given in Table IV.

The following integrals are for the nonlocal operator diagrams for the LHS of the momentum distribution.

$$\mathcal{I}_{\rho,2n}(E) = \int_q \frac{i^2 \mathbf{q}^{2n} e^{i\mathbf{q}\cdot\mathbf{r}}}{[q_0 - \frac{\mathbf{q}^2}{2m} + i\epsilon]^2} \frac{i}{E - q_0 - \frac{\mathbf{q}^2}{2m} + i\epsilon}, \quad (\text{A10})$$

$$\mathcal{I}_{\rho,0}(E) = -\frac{im^2}{8\pi\sqrt{mE}} e^{i\sqrt{mE}r} + O(1/\Lambda^3),$$

$$\mathcal{I}_{\rho,2}(E) = -\frac{im^2[\sqrt{mE} - 2i/r]}{8\pi} e^{i\sqrt{mE}r} + O(1/\Lambda).$$

-
- [1] M. Inguscio, W. Ketterle, and C. Salomon, Proc. Int. Sch. Phys. Fermi **164**, pp.1 (2007).
- [2] S. Tan, Ann. Phys. **323**, 2952 (2008), [arXiv:cond-mat/0505200](#).
- [3] S. Tan, Ann. Phys. **323**, 2971 (2008), [arXiv:cond-mat/0508320](#).
- [4] S. Tan, Ann. Phys. **323**, 2987 (2008), [arXiv:0803.0841](#).
- [5] K. G. Wilson, Phys. Rev. **179**, 1499 (1969).
- [6] L. P. Kadanoff, Phys. Rev. Lett. **23**, 1430 (1969).
- [7] A. M. Polyakov, Soviet Physics–JETP **30**, 151 (1970).
- [8] E. Braaten and L. Platter, Phys. Rev. Lett. **100**, 205301 (2008), [arXiv:0803.1125](#).
- [9] E. Braaten, D. Kang, and L. Platter, Phys. Rev. A **78**, 053606 (2008), [arXiv:0806.2277](#).
- [10] D. T. Son and E. G. Thompson, Phys. Rev. A **81**, 063634 (2010), [arXiv:1002.0922](#).
- [11] W. D. Goldberger and I. Z. Rothstein, Phys. Rev. A **85**, 013613 (2012), [arXiv:1012.5975](#).
- [12] W. D. Goldberger and Z. U. Khandker, Phys. Rev. A **85**, 013624 (2012), [arXiv:1107.1472](#).
- [13] J. Hofmann, Phys. Rev. A **84**, 043603 (2011), [arXiv:1106.6035](#).
- [14] E. Braaten, D. Kang, and L. Platter, Phys. Rev. Lett. **106**, 153005 (2011), [arXiv:1101.2854](#).
- [15] J. Hofmann, Phys. Rev. Lett. **108**, 185303 (2012), [arXiv:1112.1384](#).
- [16] Y. Nishida, Phys. Rev. A **85**, 053643 (2012), [arXiv:1110.5926](#).
- [17] E. Braaten and H.-W. Hammer, J. Phys. B **46**, 215203 (2013), [arXiv:1302.5617](#).
- [18] P. Gubler, N. Yamamoto, T. Hatsuda, and Y. Nishida, Annals Phys. **356**, 467 (2015), [arXiv:1501.06053](#).
- [19] E. Braaten, D. Kang, and L. Platter, Phys. Rev. Lett. **104**, 223004 (2010), [arXiv:1001.4518](#).
- [20] D. H. Smith, E. Braaten, D. Kang, and L. Platter, Phys. Rev. Lett. **112**, 110402 (2014), [arXiv:1309.6922](#).
- [21] E. Braaten, Lect. Notes Phys. **836**, 193 (2012), [arXiv:1008.2922](#).
- [22] F. Werner and Y. Castin, Phys. Rev. A **86**, 013626 (2012), [arXiv:1204.3204](#).
- [23] D. B. Kaplan, M. J. Savage, and M. B. Wise, Nucl. Phys. B **478**, 629 (1996), [arXiv:nucl-th/9605002](#).
- [24] U. van Kolck, Nucl. Phys. A **645**, 273 (1999), [arXiv:nucl-th/9808007](#).
- [25] Z. Yu, J. Thywissen, and S. Zhang, Phys. Rev. Lett. **115**, 135304 (2015), Erratum: Phys. Rev. Lett. **117**, 019901 (2016).
- [26] P. Zhang, S. Zhang, and Z. Yu, [arXiv:1605.05653](#).
- [27] J. Carlson, S. Gandolfi, K. E. Schmidt, and S. Zhang, Phys. Rev. A **84**, 061602 (2011).
- [28] J. Carlson, S. Gandolfi, and A. Gezerlis, PTEP **2012**, 01A209 (2012), [arXiv:1210.6659](#).
- [29] F. Werner, Phys. Rev. A **78**, 025601 (2008), [arXiv:0803.3277](#).
- [30] G. B. Partridge, K. E. Strecker, R. I. Kamar, M. W. Jack, and R. G. Hulet, Phys. Rev. Lett. **95**, 020404 (2005), [arXiv:cond-mat/0505353](#).
- [31] F. Werner, L. Tarruell, and Y. Castin, Eur. Phys. J. B **68**, 401 (2009), [arXiv:0807.0078](#).
- [32] N. Navon, S. Nascimbène, F. Chevy, and C. Salomon, Science **328**, 729 (2010), [arXiv:1004.1465](#).
- [33] E. D. Kuhnle, H. Hu, X.-J. Liu, P. Dyke, M. Mark, P. D. Drummond, P. Hannaford, and C. J. Vale, Phys. Rev. Lett. **105**, 070402 (2010), [arXiv:1001.3200](#).
- [34] G. Veeravalli, E. Kuhnle, P. Dyke, and C. J. Vale, Phys. Rev. Lett. **101**, 250403 (2008), [arXiv:0809.2145](#).
- [35] Y. Sagi, T. E. Drake, R. Paudel, and D. S. Jin, Phys. Rev. Lett. **109**, 220402 (2012), [arXiv:1208.2067](#).
- [36] J. T. Stewart, J. P. Gaebler, T. E. Drake, and D. S. Jin, Phys. Rev. Lett. **104**, 235301 (2010), [arXiv:1002.1987](#).
- [37] C. Lobo, I. Carusotto, S. Giorgini, A. Recati, and S. Stringari, Phys. Rev. Lett. **97**, 100405 (2006).
- [38] R. Combescot, S. Giorgini, and S. Stringari, EPL **75**, 695 (2006), [arXiv:cond-mat/0512048](#).
- [39] J. E. Drut, T. A. Lähde, and T. Ten, Phys. Rev. Lett. **106**, 205302 (2011), [arXiv:1012.5474](#).
- [40] S. Hoinka, M. Lingham, K. Fenech, H. Hu, C. J. Vale, J. E. Drut, and S. Gandolfi, Phys. Rev. Lett. **110**, 055305 (2013), [arXiv:1209.3830](#).
- [41] S.-Q. Su, D. E. Sheehy, J. Moreno, and M. Jarrell, Phys. Rev. A **81**, 051604 (2010).
- [42] T. Abe and R. Seki, Phys. Rev. C **79**, 054003 (2009), [arXiv:0708.2524](#).
- [43] F. Palestini, A. Perali, P. Pieri, and G. C. Strinati, Phys. Rev. A **82**, 021605 (2010).
- [44] J.-W. Chen and E. Nakano, Phys. Rev. A **75**, 043620 (2007), [arXiv:cond-mat/0610011](#).
- [45] K. Van Houcke, F. Werner, E. Kozik, N. Prokof'ev, and B. Svistunov, ArXiv e-prints (2013), [arXiv:1303.6245](#).
- [46] S. Gandolfi, K. E. Schmidt, and J. Carlson, Phys. Rev. A **83**, 041601 (2011), [arXiv:1012.4417](#).
- [47] Y. Nishida and D. T. Son, Lect. Notes Phys. **836**, 233 (2012), [arXiv:1004.3597](#).
- [48] E. Braaten, M. Kusunoki, and D. Zhang, Ann. Phys. **323**, 1770 (2008), [arXiv:0709.0499](#).